

Sedimentological Interpretation of CRP-2/2A Logs, Victoria Land Basin, Antarctica: Glacial and Sea-Level Significance

J.D. BRINK¹, R.D. JARRARD^{1*}, C. BÜCKER², T. WONIK² & F. TALARICO³

¹Dept. of Geology & Geophysics, 717 WBB, Univ. of Utah, 135 S. 1460 East, Salt Lake City - UT 84112-0111 - USA

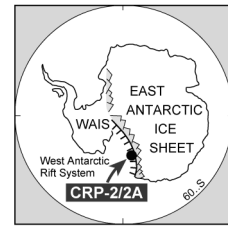
²GGA, Joint Scientific Research Institute, Stilleweg 2, 30655 Hannover - Germany

³Dipartimento di Scienze della Terra, Università degli Studi di Siena, Via del Laterano 8, 53100 Siena - Italy

*Corresponding author (jarrard@mail.mines.utah.edu)

Received 2 August 1999; accepted in revised form 18 April 2000

Abstract - Downhole changes in physical properties at CRP-2, reflecting sedimentological changes induced by glacial marine processes, are measured by a suite of well logs (density, resistivity, neutron, microresistivity, spectral gamma-ray, and magnetic susceptibility), in conjunction with a core-based limestone abundance log. The CRP-2 section is subdivided into eight log-based units. Downhole porosity changes are affected by lithology – particularly diamict - and diagenesis. Variations in spectral gamma-ray logs, in particular thorium, are correlated with core-based provenance changes throughout CRP-2. These provenance changes may link glaciation and relative sea level at CRP-2: “interglacial” erosion by glaciers of highland Ferrar Dolerite is associated with highstand sedimentation (*e.g.*, muds), whereas glacial encroachment onto lowland Granite Harbour Intrusive rocks is associated with lowstand diamicts. A sequence stratigraphic model is applied to the logs to identify sequence boundaries and systems tracts within CRP-2, independently of sequence identifications based on lithology.



INTRODUCTION

The Cape Roberts Project (CRP) is an international drilling project whose aim is to reconstruct Neogene to Palaeogene palaeoclimate by obtaining continuous core and well logs from a site near Cape Roberts, Antarctica. The first CRP drillhole, CRP-1, obtained 148 m of Quaternary and Miocene sediments (Cape Roberts Science Team, 1998). The second CRP drillhole, CRP-2, extended to 624 mbsf (metres below sea floor) with an average 94% recovery of Oligocene to Quaternary sediments (Cape Roberts Science Team, 1999).

Continuous well-log measurements were made throughout most of the CRP-2 hole. Brink & Jarrard (this volume) process and calibrate the CRP-2 logs and identify the logged portions that are reliable. Bücker et al. (this volume) analyze the CRP-2 well logs based on factor and cluster analyses. The log-based sedimentology of this paper provides a complementary perspective to these two studies and to a variety of core-based analyses presented in this volume: sequence stratigraphy, grain size variations, facies relationships, patterns of cyclicity, and provenance.

The main objective of this study is to interpret a suite of logs that measure the physical properties of CRP-2 sediments. The advantage in using well logs to analyze and interpret sedimentary history is that the logs provide multiple records of different physical properties, all of which may have geologic significance. One goal is to link detailed changes in lithology – or physical properties – with the denudation history of the Transantarctic Mountains. A second goal is the development of a log-based sequence stratigraphy. This paper is divided into six main parts: data, log physical property units, porosity changes, provenance changes, sequences, and relations among provenance, glaciation, and sea level.

DATA

Table 1 lists the CRP-2 logs used in this study. Tool descriptions are given in the CRP-2 Initial Reports (Cape Roberts Science Team, 1999). Downhole logging at CRP-2 was undertaken in three phases. The upper 200 m was logged just after the completion of drilling with HQ (96-mm diameter hole, 61-mm diameter core) drilling rod and prior to NQ (76-mm diameter hole, 45-mm diameter core) drilling. Only the interval from 63 to 165 mbsf was open-hole during this first logging run; 0-63 mbsf was cased. In the second phase the entire interval from 200 to 625 mbsf was logged open-hole. The third phase, after removal of HQ rod, was open-hole logging of the short interval 12-29 mbsf.

The magnetic susceptibility (χ) tool was run in the following open-hole intervals: 12-25, 63-167, and 200-623 mbsf. Log-based χ was calibrated to volume magnetic susceptibility (μSI) with core-plug χ measurements based on regression analysis (Brink & Jarrard, this volume).

The spectral-gamma-ray tool was run from the sea floor to 624 mbsf. The intervals 0-63 and 172-200 mbsf were logged in casing and therefore required a correction factor for attenuation effects. This correction factor was separately determined for total gamma-ray (SGR), potassium (%), and thorium (ppm), by taking the ratio of open hole versus cased median values for each element, based on a 40 metre interval where both open-hole and cased-hole data were collected.

The density tool obtained data in two open-hole intervals (12-27 and 200-440 mbsf) and one cased-hole interval (0-200 mbsf). The density data were calibrated by Bücker et al. (this volume) and then converted to a density

Tab.1 - Logs used in this study, the normal use of each log, and the specific way each log was used in the evaluation of CRP-2.

Geophysical Tool or Geological Method	Property Measured	Usual Interpretation		CRP-2 Interpretation
Spectral Gamma Ray (SGR)	Natural Radioactivity	SS vs. SH		Provenance, Sequence Stratigraphy
Magnetic Susceptibility (χ)	Magnetic Susceptibility	SS vs. SH		Provenance, Sequence Stratigraphy
Lonestone Abundance Log	Total Number of Lonestones	Diamict vs. SS/SH		Provenance, Sequence Stratigraphy, Diamict vs. SS/SH
Resistivity (ϕ_R)	Porosity	SS vs. SH	FUS & CUS	Diamict vs. SS/SH, FUS & CUS, Sequence Stratigraphy
Neutron (ϕ_N)	Porosity	SS vs. SH	FUS & CUS	Diamict vs. SS/SH, FUS & CUS, Sequence Stratigraphy
Density (ϕ_D)	Porosity	SS vs. SH	FUS & CUS	Diamict vs. SS/SH, FUS & CUS, Sequence Stratigraphy
Microresistivity (ϕ_m)	Porosity	SS vs. SH	FUS & CUS	Diamict vs. SS/SH, FUS & CUS, Sequence Stratigraphy

Abbreviations: SS=Sandstone, SH=Shale, FUS=Finning Upward Sequence, CUS=Coarsening Upward Sequence.

porosity log (ϕ_D) by assuming a constant matrix density (Brink & Jarrard, this volume). Bückler et al. (this volume) applied a casing attenuation correction factor to the interval 0-200 mbsf. Nevertheless, portions of this upper zone are probably unreliable, because it is impossible to identify and correct for washouts. The ϕ_D log for 200 to 440 mbsf provides a high-resolution porosity log, second only to microresistivity porosity, and it is strongly correlated with the three other porosity logs.

The array induction tool measures formation resistivity at three different resolutions: R_{long} , R_{medium} , and R_{short} , where R_{long} is lowest resolution and largest sampled volume. Since R_{short} is highest resolution and appears to be unaffected by hole conditions in CRP-2, it was selected by Brink & Jarrard (this volume) for conversion to formation factor and subsequently to formation-factor-based porosity (ϕ_R). The resistivity measurements were collected in the following open-hole intervals: 12-29, 63-170, and 200-623 mbsf.

The neutron tool measures total hydrogen abundance within the formation. In beds that lack hydrous minerals, hydrogen abundance is directly proportional to porosity. Bückler et al. (this volume) demonstrate that the CRP-2 neutron log includes hydrogen contributions from both porosity and clay minerals. Brink & Jarrard (this volume) convert raw neutron counts to apparent porosity (ϕ_N) by cross-plotting core-plug porosities from low-clay intervals versus raw neutron counts. Open-hole data are available from 12 to 24, 64 to 167, and 200 to 620 mbsf. In a 40-metre section of CRP-2, neutron data were collected in both open and cased hole. The ratio of open-hole to cased-hole data in this overlap interval was used for casing correction of the cased interval 167-200 mbsf.

The dipmeter log is the highest resolution log run in CRP-2. The four-pad tool, which collects conductivity measurements every 5 mm, was run in open-hole intervals from 63 to 160 and 200 to 623 mbsf. Data are missing from the interval 255-280 mbsf due to in-field software complications. Jarrard et al. (this volume) processed these data to remove low-conductivity spikes, attributed to lonestones, and to merge the four traces into a single conductivity log. Brink & Jarrard (this volume) converted this log to formation factor and subsequently to porosity (ϕ_{UR}).

Lonestone mineralogy and distribution pattern data were collected for more than 20,000 clasts from the entire 624 metres of CRP-2 core (Cape Roberts Science Team, 1999; Talarico et al., this volume). Our study employs their log of total number of lonestones per metre, using this one quantitative core-based log in conjunction with the suite of downhole logs. Although this log is lower in resolution than both the downhole logs and the CRP-1 lonestone abundance log of Brink et al. (1998), its facies usefulness is substantial (Cape Roberts Science Team, 1999).

LOG PHYSICAL PROPERTY UNITS

CRP-2 logs can be used to define eight major units, each based on changes in two or more of the following logs: ϕ_{UR} , ϕ_R , ϕ_N , ϕ_D , χ , SGR, and lonestone abundance (Fig. 1). A detailed description of log responses within and between these units is provided by Brink (1999). Geologic interpretation of these major log changes is included in following sections.

Despite several data gaps, Unit 1 (0-145 mbsf) can be characterized as exhibiting gradually decreasing porosity and increasing lonestone abundance downhole, along with gamma-ray values higher than in any other unit except Unit 3. The 145 mbsf boundary between Units 1 and 2 is marked by a sharp change to lower values in both SGR and χ logs (Fig. 1). Unit 2 (145-~200 mbsf), which has basal and capping low-gamma-ray zones, generally contains the lowest lonestone abundances of the entire CRP-2 hole (0-10 ls/m). Unit 3 (~200-273 mbsf) apparently begins at 200 mbsf, but it may begin earlier within the cased interval from 165-200 mbsf. The SGR log within Unit 3 is the highest and most uniform of the entire hole, and porosities are ~35% from 200 to 245 mbsf, steadily increasing to a peak of ~45% at 260 mbsf. Unit 4 (273-328 mbsf) includes sharply lower SGR than Unit 3, and susceptibilities that are distinctly lower than in any other unit. Unit 5 (328-350 mbsf) is a short interval that exhibits a sudden increase to high and relatively constant SGR and χ . Unit 6 (350-445 mbsf) contains the highest overall abundance of lonestones of any unit; most of the unit

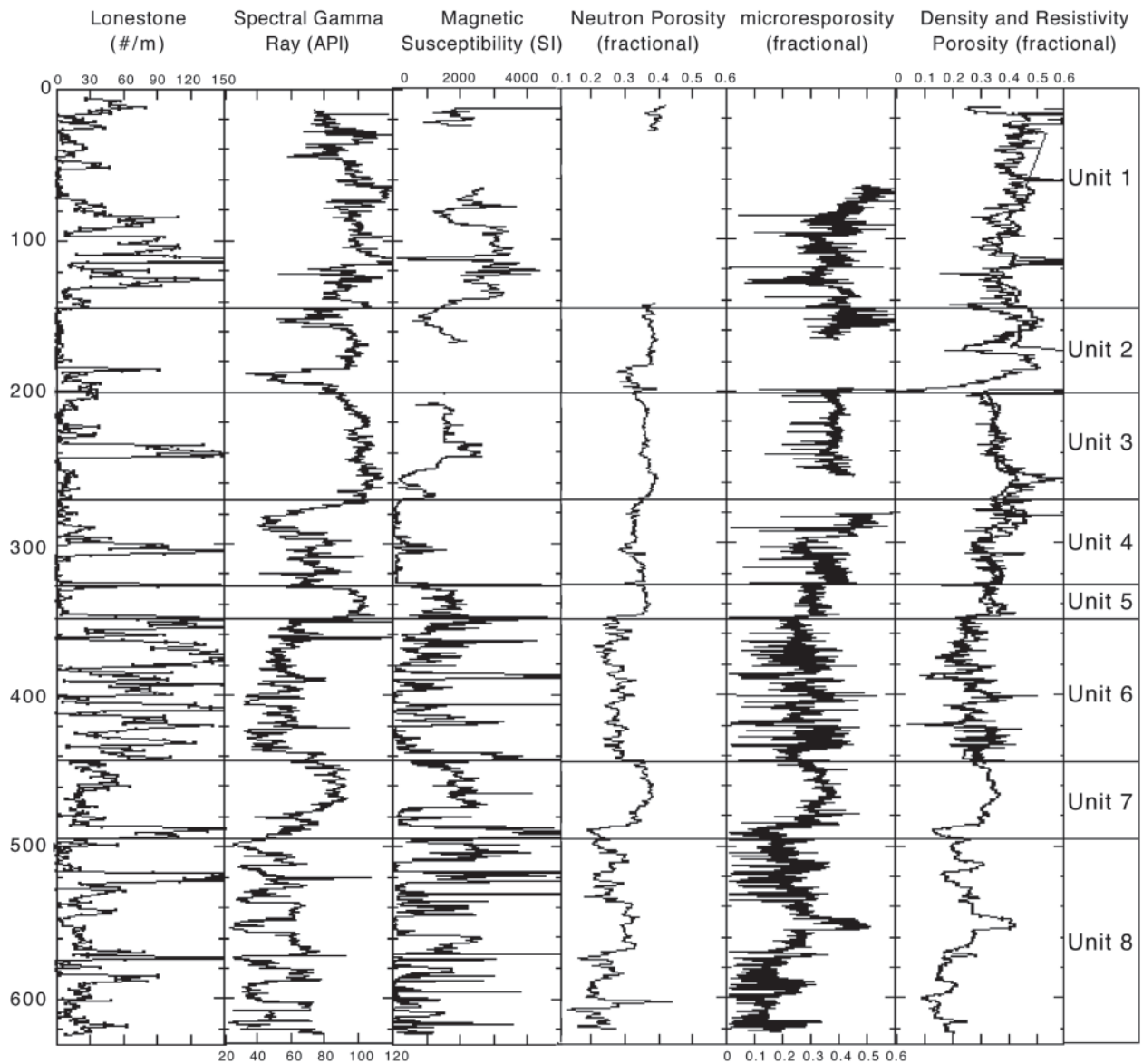


Fig. 1 - Lonestone abundance, spectral gamma-ray, magnetic susceptibility, neutron-porosity, microresistivity porosity, density-porosity, and shallow resistivity-porosity logs for CRP-2, along with log-based units and unit boundaries. The criterion for selecting units is a dramatic downhole change in at least two of the CRP-2 logs, compared to the overlying unit; this change may be either in average value or in log character (e.g., heterogeneity).

contains 50-150 ls/m. High lonestone abundances correlate with spiky χ character, ranging from 100 to >5000 mSI over a depth of <10 metres, and heterogeneous porosities. In contrast to Unit 6, Unit 7 is relatively homogeneous, higher in porosity and gamma ray, and lower in lonestone abundance. Unit 8 (495-625 mbsf) is the only unit in CRP-2 characterized by bimodal and usually covariant c and SGR. Unit 8 porosities are generally low.

POROSITY CHANGES

RESPONSE TO LITHOLOGY

Porosities of sediments at CRP-1 and CRP-2 are affected by both lithology and postdepositional modifications such as compaction, fracturing, and diagenesis. Of particular interest for our analysis is the usefulness of porosity as a lithology indicator.

The normally expected distinction between shale (mudstone) and sandstone porosities is often subtle within both CRP-1 (Niessen et al., 1998; Niessen & Jarrard, 1998) and CRP-2 (Brink & Jarrard, this volume; Niessen et al., this volume). In general, CRP-2 mudstones are slightly higher in porosity than sandstones. In many intervals, mudstones can be identified based on significantly higher porosities (e.g., 144-160 mbsf versus 130-138 mbsf in Fig. 1). However, their porosities can be similar (e.g., 535-544 mbsf versus 527-535 mbsf), and sandstones rarely are actually higher in porosity than mudstones (e.g., 504-508 mbsf versus 510-516 mbsf). Mechanical compaction cannot generate such variations; diagenesis must be responsible.

Both sands and muds are consistently higher in porosity than diamicts, at both CRP-1 (Niessen & Jarrard, 1998) and CRP-2 (Niessen et al., this volume). Diamicts, found mainly in lowstand systems tracts (see section on sequences), generally exhibit distinctly lower porosities

than adjacent sediments. This porosity decrease is probably caused mostly by poor sorting of diamicts, which may include clay-size to boulder-size grains (Cape Roberts Science Team, 1999). Glacial overconsolidation cannot account for low diamict porosities, because the porosities of underlying units also would be reduced. Diamict facies are identifiable in CRP-2 logs both by their low porosity and by high lonestone abundance and χ . Diamicts by definition include lonestones, and abundant magnetic minerals within these lonestones cause high susceptibilities.

DIAGENESIS

Carbonate cementation affects the CRP-2 logs mainly by reduction of porosity. Carbonate content increases downhole, from ~1% in the top 100 m to 3-6% below 440 mbsf (Dietrich, this volume). Accordingly, sandstone and mudstone porosities in the lower part of the hole are 5-10% lower than expected based on the overall CRP-2 compaction pattern (Brink & Jarrard, this volume). Cementation is most intense below 500 mbsf, where calcite mineralization appears to be composed of different generations of cementation (Cape Roberts Science Team, 1999; Aghib et al., this volume).

Cementation in CRP-2 is observable in all porosity logs, but it is most apparent in the high-resolution microresistivity porosity log (Fig. 1). Above 350 mbsf, microresistivity spikes to low porosity are more rare than below 350 mbsf; these spikes are usually attributable to individual large lonestones and more rarely to thin cemented beds. Within Unit 6 (350-445 mbsf), spikes to both high and low porosity are very abundant. Because this unit is much richer in lonestones and diamicts than other portions of CRP-2, it is not possible to isolate diagenetic from lithologic and clast effects on porosity. Porosity is relatively high and free of cemented beds within most of Unit 7 (445-485 mbsf). Spikes to near-zero porosity increase dramatically below 485 mbsf, the same depth at which sedimentologists observe the most intensive cementation. Below 485 mbsf, these zones appear to be most pervasively cemented: 485-536, 570-602, and 612-622 mbsf. The occasional juxtaposition of nearby cemented and unconsolidated (leached?) sands, like similar observations at CRP-1 (Cape Roberts Science Team, 1998) and CIROS-1 (Bridle & Robinson, 1989), attests to the variability of carbonate saturation for fluid flow through these sites.

PROVENANCE CHANGES

INTRODUCTION

The source region for sediments found at CRP-2 is the Transantarctic Mountains (Cape Roberts Science Team, 1999; Barrett et al., 1981; Barrett et al., 1995; Bellanca et al., this volume; Smellie, this volume; Talarico et al., this volume). Source rocks include sandstones of the Beacon Supergroup (Devonian to Jurassic), Ferrar dolerites (Jurassic), Kirkpatrick basalts (Jurassic), granitoids of the Granite Harbour Intrusive Complex (Cambro-Ordovician),

and alkaline rocks from the McMurdo Volcanic Group (late Cenozoic). The main sediment distribution path for sediments at CRP-2 is through Granite Harbour streams and glaciers.

The broad pattern of provenance changes within CRP-2 has been identified by recognition of lonestone clast types (Talarico et al., this volume), whole-rock geochemistry (Krissek & Kyle, this volume; Bellanca et al., this volume), microscopic examination of rock thin sections and smear slides (Smellie, this volume; Polozek, this volume), and X-ray diffraction analysis of the silt and clay fractions (Ehrmann, this volume; Neumann & Ehrmann, this volume). Here, we use spectral gamma-ray logs as provenance indicators. Comparison of these logs with core-based changes in provenance can provide information useful for interpretation of the denudation history of the Transantarctic Mountains.

CORE-BASED PROVENANCE

Based on the distribution of clast types, seven main petrofacies were identified in CRP-2 (Cape Roberts Science Team, 1999; Talarico et al., this volume). Some petrofacies have associated log responses (Brink, 1999), particularly in χ and SGR, but only two petrofacies boundaries coincide with log-based unit boundaries (~150 and ~440 mbsf).

For most of the hole, the dominant source region for both lonestones and finer sediments is either Granite Harbour Intrusive Complex or Ferrar Dolerite. A useful indicator of changes in these sources is the relative proportion of Granite Harbour Intrusive (GHI) and Ferrar Dolerite (FD) lonestones: GHI/(GHI+FD) (Cape Roberts Science Team, 1999; Talarico et al., this volume; Fig. 2). The gradual uphole increase in GHI/(GHI+FD) is thought to reflect long-term uplift and erosion of the Transantarctic Mountains: initially exposed rocks of the adjacent mountains consisted almost entirely of Ferrar Dolerite and Beacon Supergroup, but erosion of these rocks increasingly exposed underlying Granite Harbour Intrusive Complex to erosion (Cape Roberts Science Team, 1999; Talarico et al., this volume). In the lower third of CRP-2, the abundant Ferrar Dolerite lonestones are locally accompanied by clasts of Beacon sandstone. A fourth lonestone source, basaltic volcanism of the McMurdo Volcanic Group, is first detected at about 310 mbsf and is generally abundant above 280 mbsf (Cape Roberts Science Team, 1999; Talarico et al., this volume).

Changes in bulk mineralogy and sand mineralogy are compatible with these patterns in lonestone provenance. Down to 280 mbsf the sand fraction consistently contains components derived from the McMurdo Volcanic Group as well as green hornblende from the Granite Harbour Intrusives (Smellie, this volume). Below 300 mbsf, bulk mineralogy and sand composition show a pattern of decrease in feldspar/quartz and K-feldspar/quartz ratios (Cape Roberts Science Team, 1999). McMurdo Volcanic detritus is replaced by fine-grained dolerite in the sand fraction, and Ferrar dolerite clasts are generally more abundant than Granite Harbour Intrusive clasts. A major change in maturity occurs at 300 mbsf: above this depth

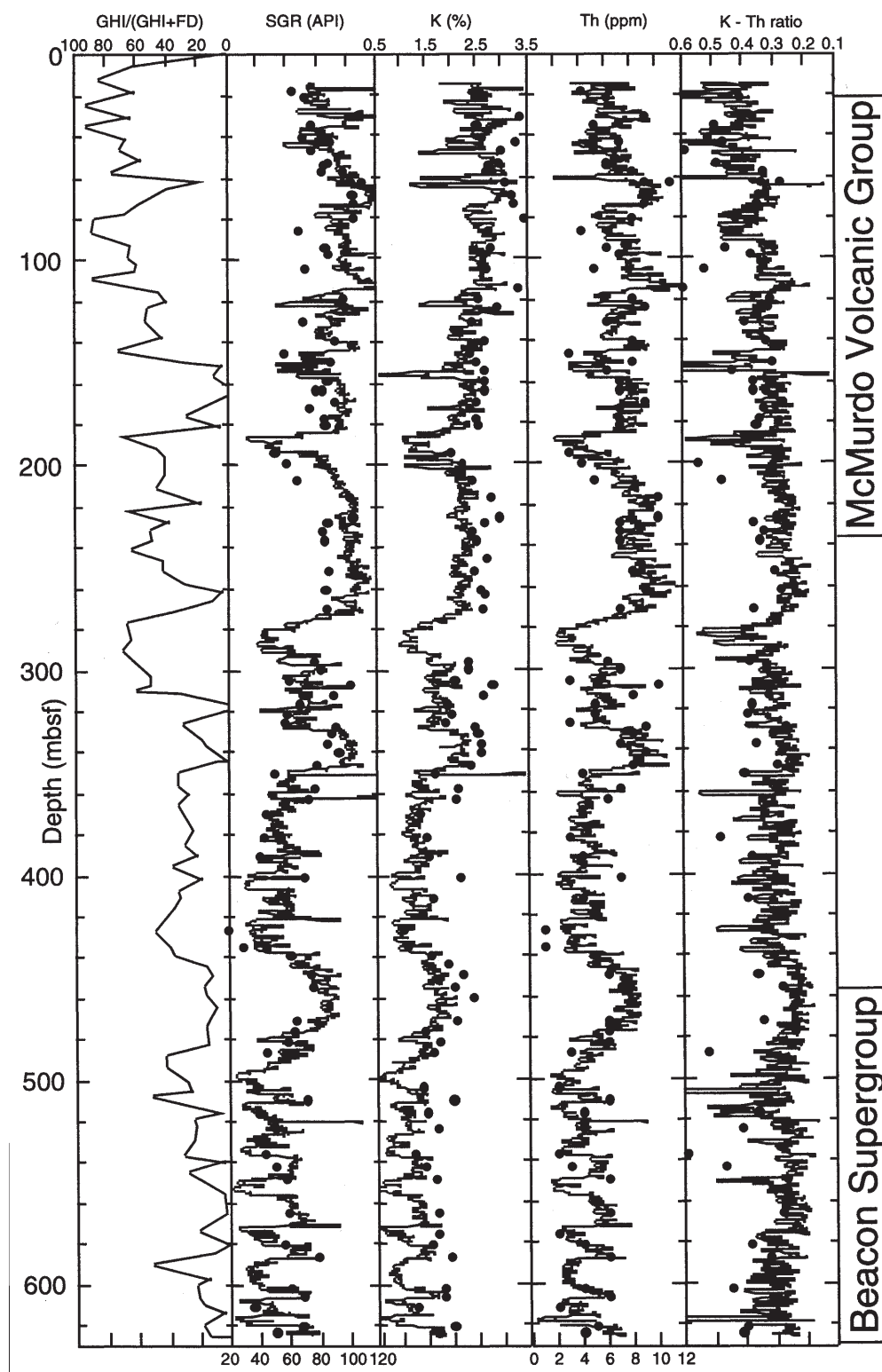


Fig. 2 - Lonestone provenance, indicated by the ratio $GHI/(GHI+FD)$ (Cape Roberts Science Team, 1999; Talarico et al., this volume), compared to spectral gamma-ray, potassium, thorium, and potassium/thorium ratio logs. Also plotted are core-based geochemical measurements of potassium and thorium (Kyle, personal communic., 1999; Krissek & Kyle, this volume). The similarity in high-frequency character between the gamma-ray plots and the provenance plot demonstrates that gamma-ray can be used as a high-resolution provenance indicator.

grains are variably abraded and are sub-angular to sub-rounded, whereas below 300 mbsf the abundance of rounded grains increases significantly, indicating a Beacon sandstone source (Smellie, this volume). These patterns suggest a downhole change in provenance from crystalline basement and the McMurdo Volcanics to Beacon Supergroup and Ferrar sources.

LOG-BASED PROVENANCE

In many sedimentary environments, the gamma-ray log (SGR) can be used to identify shales and sandstones and to estimate shale content. Similarly, the magnetic susceptibility log (χ) can also be used to distinguish finer-grained mudstones from coarser-grained sandstones, by

detecting magnetic minerals that are generally found in the finer-grained sediments. The combination of SGR and χ logs therefore usually provides a robust indicator of sandstone versus shale. In CRP-2, however, both logging tools respond not only to sand/shale but also to provenance.

The magnetic susceptibility log is unreliable as a sand/shale indicator when magnetic minerals are not confined to the fine-grained shales. Studies of the CIROS-1 and CRP-1 cores showed that changes in magnetic susceptibility are primarily due to changes in the concentration of pseudo-single domain magnetite and that these changes may be environmentally controlled (Cape Roberts Science Team, 1999; Sagnotti et al., 1998a, 1998b). For CRP-2, comparison of χ and lonestone abundance logs suggests that χ spikes in the lower 300 m are related to the occurrence of lonestones (see Fig. 1). Niessen et al. (1998) observed a similar association within CRP-1.

SGR-based identifications of sands and shales become suspect if potassium feldspar, mica, heavy minerals, or other sources of radioactivity are present in substantial quantities within the sandstones. Recognizing this possibility, we ran a spectral gamma-ray tool in CRP-2, determining potassium (K), thorium (Th), and K/Th ratio in addition to SGR. These logs demonstrate that provenance is as important as sand/shale in generating variations in the CRP-2 gamma-ray logs. Reliability of the K and Th logs is confirmed by comparison to geochemical analyses of 97 CRP-2 samples (Kyle, personal communication, 1999; Krissek and Kyle, this volume) (Fig. 2).

The McMurdo Volcanic Group is rich in radioactive elements, particularly in K, and consequently gamma-ray response increases in the upper 300 m. MVG influx above 275 mbsf causes a gradual uphole increase in K and increase in K/Th, as well as an upward baseline shift at ~275 mbsf (the Unit 3/4 boundary) in all four gamma-ray logs (Fig. 2). The contribution of clay minerals to total radioactivity within Unit 3 appears to be overwhelmed by the radioactivity of volcanic clasts and volcanic sands, preventing the identification of sandstone and shale baselines. Diamicts, mudstones, and sandstones are all represented within this high gamma-ray interval.

Below ~280 mbsf, SGR values are generally lower and more variable than above this depth (Fig. 2). Below 500 mbsf, the dominating effect of immature and volcanic mineralogy is no longer apparent: gamma-ray responses are bimodal, with very low values for the lower mode. The low gamma-ray intervals are generally sandstones, and their lack of radioactivity indicates that they are relatively clean. Quartz from the Beacon sandstones is the most likely source of these clean sands. The SGR record below 500 mbsf is a reasonably good grain size indicator, as in many other marine sedimentary environments. Even here, however, SGR sometimes detects an additional component, increased SGR in intervals rich in lonestones.

Most of the short-term (40-80 m) cycles in lonestone provenance (GHI/(GHI+FD)) have correlative gamma-ray responses (Fig. 2). Thorium, which is the dominant variable controlling the total gamma-ray log, appears to be the best proxy for GHI/(GHI+FD) (Fig. 2). Increased Granite Harbour Intrusive component is recorded as a decrease in thorium, whereas increased Ferrar Dolerite

causes an increase in thorium.

In summary, long-term changes in gamma-ray logs (particularly potassium) are most sensitive to temporal variations in contributions from the McMurdo Volcanic Group and Beacon sandstones. In contrast, shorter-term changes (particularly in thorium) reflect relative proportions of Granite Harbour Intrusive Complex and Ferrar Dolerite.

SEQUENCES

CORE-BASED SEQUENCES

Sedimentologists and stratigraphers of the Cape Roberts Science Team (1999) have identified 25 disconformity-bounded, glacial-marine, depositional sequences in CRP-2. The process of determining sequence boundaries and sequence types was based on the method of Fielding et al. (1998). The assumption is that grain-size changes reflect changes in depositional energy and therefore generally coincide with changes in palaeobathymetry. However, other depositional processes (*e.g.*, slumps, turbidity currents) can complicate this association. Sequences typically are composed of four elemental sediment packages from bottom to top: (1) a poorly sorted coarse-grained unit (2-20 m thick) composed of diamict, pebbly sandstone, or conglomerate and lying upon a sharp-based unconformity; (2) a fining upward unit (up to 25 m thick) of sandstone fining into sandy mudstone; (3) a mudstone (up to 30 m thick) grading into a muddy sandstone and then to a sandstone-dominated lithology (up to 20 m thick); and (4) a sharp-based, well sorted, massive to cross-bedded sandstone and/or interbedded sandstones and siltstones (2-10 m thick).

Geologic interpretation of these 25 sequences is presented in the CRP-2 Initial Reports (Cape Roberts Science Team, 1999) and by Fielding et al. (this volume). One goal of this paper is to compare and contrast core-based sequence identification with log data (Fig. 1), both well logs and core lonestone abundance. Although geological interpretation of the logs is often less certain than core interpretation, the log data have the advantages of being continuous, high resolution, and capable of quantitatively detecting subtler variations in porosity and clay content than those identifiable through visual core descriptions.

LOG IDENTIFICATION OF SEQUENCE BOUNDARIES AND SYSTEM TRACTS

One-dimensional sequence stratigraphic analysis, whether based on cores or well logs, can be difficult and ambiguous. Often, systems tract boundaries have a subtle expression on logs, and they may be impossible to recognize in cores (Emery & Myers, 1996). Historically, gamma-ray, sonic, SP, density, neutron, and resistivity logs have been the primary logs used for well-log interpretation of sequences (Emery & Myers, 1996). We undertake CRP-2 sequence boundary and systems tract analysis by analyzing porosity-sensitive logs (ϕ_N , ϕ_R , ϕ_D , and ϕ_μ) and lithologic-sensitive

logs (SGR, χ , and lonestone abundance). Recognition of sequence boundaries and other significant surfaces is followed by a subdivision into systems tracts. Identification of the systems tracts allows them to be placed in the context of transgressive/regressive cycles (Emery & Myers, 1996). The sequence stratigraphic model and terminology employed in this paper are similar to the models described by Cape Roberts Science Team (1999), Naish & Kamp (1997), Emery & Myers (1996), and Van Wagoner et al. (1990). However, the extent to which low-latitude sequence stratigraphic models are appropriate to glacial environments such as CRP is uncertain (Cape Roberts Science Team, 1998, 1999; Fielding et al., this volume; Powell et al., this volume).

In most siliciclastic marine environments, both porosity-sensitive logs (ϕ_N , ϕ_R , ϕ_D) and lithologic-sensitive logs (SGR and χ) are utilized as grain-size indicators. Sands and muds have quite different initial porosities due to differences in grain packing, and lithification to sandstones and shales modifies their porosities without removing the porosity difference. Individual porosity logs can provide a clear record of grain size changes in normally compacted, cement-free intervals of CRP-2. Large-scale porosity trends can be identified on the ϕ_N , ϕ_R , and ϕ_D logs, whereas the microresistivity log provides a high-resolution record of smaller-scale porosity changes. In all CRP-2 porosity logs, several variables other than grain size locally affect porosity: (1) diamicths have low porosity; (2) diagenetic effects such as carbonate cementation also decrease porosity; (3) open fractures (or washouts) increase porosity in the high-resolution dipmeter response; (4) overcompaction due to the overriding of glaciers (Cape Roberts Science Team, 1999) may add to normal consolidation effects and decrease porosity. Fine-grained sediments are usually much higher in magnetic and radiogenic minerals than coarse-grained sediments, and they are therefore also higher in SGR and χ response. Provenance changes in CRP-2 often mask the record of grain size changes within SGR (see section on provenance change). However, individual facies, in particular diamicths, may have unique properties identifiable in SGR and χ logs. Because neither the porosity logs nor the lithological logs are universally diagnostic for recognition of grain-size variations within CRP-2, we use them in combination.

Log-based sequence boundaries include 22 of the 25 core-based sequence boundaries and two additional sequence boundaries not previously identified. Core-based CRP sequence boundaries typically separate underlying mudstones, siltstones, or sandstones from overlying diamicths. This transition to diamicths is usually evident in several logs (Fig. 3). The most obvious log indicator is increased lonestone abundance, since by definition diamicths contain increased proportions of lonestones. It is not unusual to see an increase from <5 to >150 ls/m across a sequence boundary.

Susceptibility values in diamicth units are generally high, in association with the increased number of clasts. The χ log detects the increased abundance of magnetic minerals in igneous and metamorphic lonestones. A complicating factor is that some increases in lonestone abundance are not identified as sequence-bounded diamicths

and yet show similar χ responses to sequence boundaries. Furthermore, some lonestone peaks are relatively nonmagnetic, probably because many of the clasts are sedimentary (Beacon sandstone) rather than igneous (Ferrar Dolerite) or metamorphic (Granite Harbour) (Cape Roberts Science Team, 1999).

SGR values also appear to be sensitive to physical property changes at sequence boundaries. However, the correlation is not as clear as with the χ log, in part because the uppermost sediments in a sequence may be either sands or muds. At least six sequence boundaries are marked by a substantial decrease in gamma-ray values. However, the SGR response at many other sequence boundaries appears to be masked by immature sediments.

Nearly all sequence boundaries are accompanied by a decrease in porosity. This decrease probably is not attributable to basal till deposited by an overriding glacier, because glacial overconsolidation would also affect sediments immediately below the sequence boundary. The low porosity of these diamicths is probably attributable to their poor grain-size sorting.

The lowstand systems tract (LST) in CRP-2 is recognized in cores as a diamicth, sandstone, or conglomerate unit overlying a sequence boundary (Cape Roberts Science Team, 1999). This coarse-grained basal facies is interpreted as having an origin that represents ice-proximal deposition during advance and retreat of glacier ice in a shallow marine setting (Cape Roberts Science Team, 1999). The LST is recognized as a lonestone-rich unit in the lonestone abundance log. An associated χ high and ϕ low also demarcate the LST. SGR values are low in the LST, unless provenance dominates.

The boundary between the LST and the transgressive systems tract (TST), the transgressive surface, is generally difficult to identify in the CRP-2 core (Cape Roberts Science Team, 1999). However, this boundary and subsequent TST are commonly observable as a distinct change in slope of several of the logs. Frequently the TST can be identified as an increase in porosity which represents a fining upward sequence. The SGR and χ logs can also indicate a fining upward sequence if lonestones or provenance changes do not dominate their responses. Lonestone abundance generally decreases within the TST. In some of the sequences it is not possible to distinguish between the LST and TST.

The highstand systems tract (HST) is typically separated from the underlying TST by a maximum flooding surface. This surface may occur at the base of a condensed section, which is identified in the core as a fossiliferous mudstone (Cape Roberts Science Team, 1999). The condensed section is most extensive at the time of maximum regional transgression of the shoreline and commonly contains the most abundant, diverse faunal assemblages due to decreased terrestrial input (Loutit et al., 1988; Van Wagoner et al., 1990). The maximum flooding surface is frequently a SGR and χ high; minimum lonestone abundance and a ϕ maximum also characterize a deep-water flooding surface. The HST represents the point in a cycle just before, during, and after a relative sea-level maximum. For this reason it is common to find a "bow shaped" pattern in SGR, χ , and ϕ , signifying the change from a regressive

Depth (mbsf)	Sequence Boundaries	Systems Tracts	Lowstand Systems Tract	Trans. Systems Tract	Maximum Flooding Surface	Highstand Systems Tract	Regressive Systems Tract
Depth (mbsf)	ϕ_n ϕ_R ϕ_μ ϕ_D L_s X GR	Systems Tracts	GR X L_s ϕ	GR X L_s ϕ	GR X L_s ϕ	GR X L_s ϕ	GR X ϕ
25	Sequence 1 no x x na x ? x	?	GR X Ls ϕ	GR X Ls ϕ	GR X Ls ϕ	GR X Ls ϕ	GR X ϕ
50	Sequence 4 na na na x x na no	?	GR X Ls ϕ	GR X Ls ϕ	GR X Ls ϕ	GR X Ls ϕ	GR X ϕ
75	Sequence 5 na ? x ? x no no	HST MES TST	GR X Ls ϕ	GR X Ls ϕ	GR X Ls ϕ	GR X Ls ϕ	GR X ϕ
100	Sequence 7 na x x no x ? no	LST HST MFS LST HST?	GR X Ls ϕ	GR X Ls ϕ	GR X Ls ϕ	GR X Ls ϕ	GR X ϕ
125	Sequence 8 na x x ? x no no	LST RST	GR X Ls ϕ	GR X Ls ϕ	GR X Ls ϕ	GR X Ls ϕ	GR X ϕ
150	Sequence 9	HST?	GR X Ls ϕ	GR X Ls ϕ	GR X Ls ϕ	GR X Ls ϕ	GR X ϕ
175	X na na ? x na ?	LST/TST	GR X Ls ϕ	GR X Ls ϕ	GR X Ls ϕ	GR X Ls ϕ	GR X ϕ
200	Sequence 10	HST/ RST?	GR X Ls ϕ	GR X Ls ϕ	GR X Ls ϕ	GR X Ls ϕ	GR X ϕ
225	?	LST/TST	GR X Ls ϕ	GR X Ls ϕ	GR X Ls ϕ	GR X Ls ϕ	GR X ϕ
250	Sequence 11 ? ? x x x x no	HST/RST? MES TST	GR X Ls ϕ	GR X Ls ϕ	GR X Ls ϕ	GR X Ls ϕ	GR X ϕ
275			GR X Ls ϕ	GR X Ls ϕ	GR X Ls ϕ	GR X Ls ϕ	GR X ϕ
300	X X X X X X X X	LST	GR X Ls ϕ	GR X Ls ϕ	GR X Ls ϕ	GR X Ls ϕ	GR X ϕ
325	Sequence 12 X X X X X X ?	HST/ RST LST HST MFS TST LST	GR X Ls ϕ	GR X Ls ϕ	GR X Ls ϕ	GR X Ls ϕ	GR X ϕ
350	Sequence 13 X ? X X X X X	?	GR X Ls ϕ	GR X Ls ϕ	GR X Ls ϕ	GR X Ls ϕ	GR X ϕ
375	Sequence 14 X X X X X ? no	HST/ RST LST MFS TST	GR X Ls ϕ	GR X Ls ϕ	GR X Ls ϕ	GR X Ls ϕ	GR X ϕ
400	Sequence 15 a X X X X X X ?	HST/ RST LST MFS TST	GR X Ls ϕ	GR X Ls ϕ	GR X Ls ϕ	GR X Ls ϕ	GR X ϕ
425	Sequence 16 X X X X X X no	HST/ RST LST MFS TST	GR X Ls ϕ	GR X Ls ϕ	GR X Ls ϕ	GR X Ls ϕ	GR X ϕ
450	Sequence 17 X X X X X X X	HST/ RST LST MFS TST	GR X Ls ϕ	GR X Ls ϕ	GR X Ls ϕ	GR X Ls ϕ	GR X ϕ
475	Sequence 18 a X X X X X X X	HST/ RST LST MFS TST	GR X Ls ϕ	GR X Ls ϕ	GR X Ls ϕ	GR X Ls ϕ	GR X ϕ
500	Sequence 18 b X X X X X X X	HST/ RST LST MFS TST	GR X Ls ϕ	GR X Ls ϕ	GR X Ls ϕ	GR X Ls ϕ	GR X ϕ
525	Sequence 19 X X X na X X no	LST	GR X Ls ϕ	GR X Ls ϕ	GR X Ls ϕ	GR X Ls ϕ	GR X ϕ
550	Sequence 20 X X X na X X X	HST/RST TST LST	GR X Ls ϕ	GR X Ls ϕ	GR X Ls ϕ	GR X Ls ϕ	GR X ϕ
575	Sequence 21 no X X na ? no X	HST/ RST? TST MFS	GR X Ls ϕ	GR X Ls ϕ	GR X Ls ϕ	GR X Ls ϕ	GR X ϕ
600	Sequence 22 X no X na X X X	LST RST MFS TST	GR X Ls ϕ	GR X Ls ϕ	GR X Ls ϕ	GR X Ls ϕ	GR X ϕ
625	Sequence 23 X X na X X X	HST/ RST LST MFS TST	GR X Ls ϕ	GR X Ls ϕ	GR X Ls ϕ	GR X Ls ϕ	GR X ϕ
	Sequence 24 no X na X X X	HST/ RST LST MFS TST	GR X Ls ϕ	GR X Ls ϕ	GR X Ls ϕ	GR X Ls ϕ	GR X ϕ
	Sequence 25 X no X na X X X	HST/ RST LST MFS TST	GR X Ls ϕ	GR X Ls ϕ	GR X Ls ϕ	GR X Ls ϕ	GR X ϕ

Fig. 3 - Log-based identifications of sequences and systems tracts. Criteria used include characteristic responses on gamma-ray (GR), susceptibility (X), lonestone abundance (Ls), and porosity (ϕ) logs, as described in the text.

interval to a prograding interval (Emery & Myers, 1996). Lonestone abundances that are low or gradually decreasing can also be common in the HST.

Although the progradational interval mentioned above is typically included in the HST (Van Wagoner et al., 1990; Emery & Myers, 1996), the Cape Roberts Science Team (1999) has suggested that this interval be referred to as the regressive systems tract (RST) after Naish & Kamp (1997). It is not uncommon for the change from HST to RST to be gradual and indistinguishable. However, in several sequences there is a marked change in the slope of the logs that is interpreted as the boundary between the HST and the more progradational RST. The RST frequently exhibits a decrease in SGR, χ , and ϕ , indicating a coarsening upward sequence.

Figure 3 summarizes the log-based identifications of sequence boundaries and systems tracts, along with the diagnostic logs for each. Brink (1999) provides 100-m per page logs that document the detailed variations in log character – including coarsening and fining upward patterns – associated with all inferred sequence boundaries and systems tracts.

Following log-based identification of sequences, these sequences were numbered (Fig. 3) based on comparison to – and modification of – the core-based sequence identifications (Cape Roberts Science Team, 1999; Fielding et al., this volume). Figure 4 compares sequence and system tract identifications based on logs to those based on cores (Cape Roberts Science Team, 1999). The two sequence stratigraphies are based on mostly – but not entirely – independent data; core-based lonestone abundances are considered in both. The sequence boundary identifications based on the two methods are usually the same, with a few exceptions. Sequences identified by CRP stratigraphers in the upper 40 m are not evident in the logs; log-based identification of sequences in the upper 65 m is difficult due to the paucity of logs. We suggest that two core-based sequences (15 and 18) each may be subdivided into two sequences based on log responses. That the sequence stratigraphies generally agree is not surprising, given that they are based on the same sedimentological model. This agreement does increase confidence in the admittedly subjective process of sequence and systems tract identification, as well as in the interpreted log responses. It does not, however, test the reliability of the underlying sequence stratigraphic model. Discrepancies are also useful (except where attributable to minimal log data) as indicators of locations where our assumptions may be suspect.

PROVENANCE, GLACIATION, AND SEA LEVEL

Provenance variations at CRP-2 include both long-term and high-frequency patterns. The long-term change from Beacon and Ferrar to Granite Harbour sources is caused by uplift and erosion of Transantarctic Mountains (Cape Roberts Science Team, 1999; Talarico et al., this volume), as previously discussed. Superimposed on this long-term trend are high-frequency (40-80 m) cycles that cannot be attributed to gradual mountain denudation.

Instead, they require fluctuations within the Granite Harbour drainage basin in either erosion or transport. Figure 5B demonstrates that lonestone GHI/(GHI+FD) variations are correlated with lithology: the lonestone assemblage within diamicts is enriched in Granite Harbour Intrusives, in contrast to a Ferrar-enriched assemblage in the mudstones.

This correlation between lonestone GHI/(GHI+FD) and matrix lithology may reflect erosional patterns in the Transantarctic Mountains as a function of local sea-level change. Ferrar Dolerite, which overlies the Granite Harbour Intrusives, occupies the Transantarctic Mountain highlands, whereas the lowlands consist of Granite Harbour Intrusives (Fig. 6). During relatively warm “interglacials”, glaciers are usually confined to the highlands and therefore erode mostly Ferrar Dolerites. The association of Ferrar-rich provenance with offshore muds appears to imply a relationship between interglacials and locally high sea levels. During glacial periods, in contrast, glaciers frequently advance through the Granite Harbour lowlands and therefore a greater proportion of Granite Harbour Intrusives is eroded. An associated drop in relative sea-level along with greater proximity to the ice sheet favors deposition of diamicts at CRP-2. Thus both glacial and interglacial provenance may be controlled by glaciation patterns. Associated change in relative sea level, as inferred from sedimentary facies and sequence stratigraphy, links high sea levels to interglacials and low sea levels to glacial periods.

Logs provide a different perspective on this hypothesized pattern. As discussed in a previous section, the high-frequency fluctuations in lonestone provenance are generally correlated with cycles in the thorium log (Fig. 5A). Some exceptions are evident, attributable to local influxes of McMurdo Volcanic Group (top 280 m) or Beacon sandstones (bottom 120 m). This correlation implies that the provenance variations are not confined to the lonestones; bulk-rock chemistry (and presumably mineralogy) is similarly affected. An association among lonestone provenance, bulk-rock chemistry, and sand provenance is well established for CRP-2 (Cape Roberts Science Team, 1999; Bellanca et al., this volume; Krissek & Kyle, this volume; Neumann & Ehrmann, this volume; Polozek, this volume; Smellie, this volume), but sampling density had limited demonstration of this association to long-term trends. The correlation between GHI/(GHI+FD) and the thorium log indicates that this log can be used as a useful – albeit imperfect – high-resolution proxy for provenance fluctuations. Total gamma-ray and potassium logs are slightly less useful, because McMurdo Volcanic Group is high enough in potassium to generate some of the character in both of these logs.

If provenance change due to glacial/interglacial cycles is also associated with sea-level cycles, then generally higher thorium values may be expected for highstands than for lowstands. This prediction is confirmed (Fig. 5C) for 12 of 13 confidently identifiable pairs of highstand (HST) and lowstand systems tracts (LST), a pattern that is statistically significant at the 99% confidence level. This approach minimizes the tendency for variations in McMurdo Volcanics to obscure sea-level-controlled changes in provenance, because volcanic eruptions are

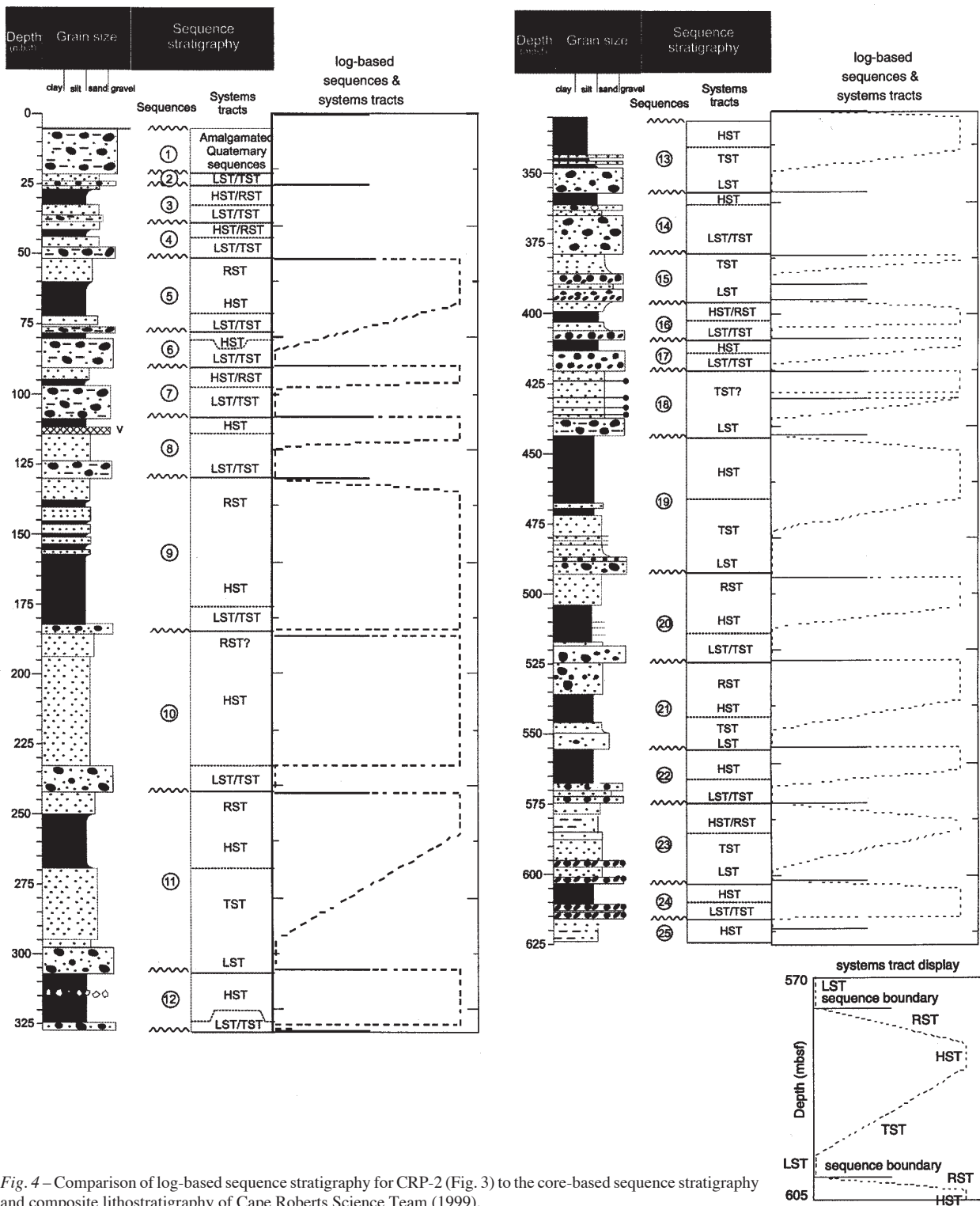


Fig. 4 – Comparison of log-based sequence stratigraphy for CRP-2 (Fig. 3) to the core-based sequence stratigraphy and composite lithostratigraphy of Cape Roberts Science Team (1999).

unrelated to sea level. Consequently, the HST thorium values are higher than LST values within the same sequence but not necessarily amongst all sequences. A similar pattern is evident in the K/Th ratio log. HST K/Th values are lower than LST values within 11 of 13 sequences (Fig. 5D), a pattern that is statistically significant at the 95% confidence level. The advantage of K/Th is that it is insensitive to Beacon sandstones, which are locally abundant below 500 mbsf. Whereas Beacon quartz concentrations in this lower interval could account for the

pattern of lower thorium in lowstand diamicts than in highstand clay-rich (thorium-rich) muds, K/Th is unaffected by Beacon dilution. Furthermore, many CRP-2 highstand deposits are silts or sands rather than muds (Cape Roberts Science Team, 1999; Fig. 4). Both the thorium and K/Th logs add further confirmation that during times of base level drop, when diamicts are deposited at or near the CRP-2 site, an influx of sediments derived from Granite Harbour Intrusives occurs.

CRP-2 sequence boundaries coincide with glacial

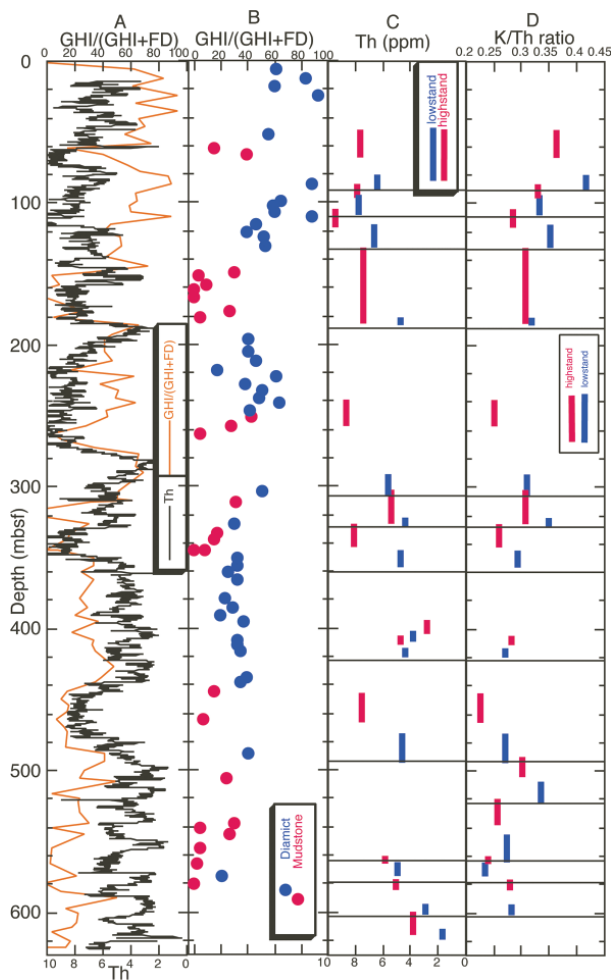


Fig. 5 - (A) GHI/(GHI+FD) lonestone provenance index overlain on the thorium (ppm) log, demonstrating ability of the thorium response to indicate high-frequency (<60 m) variations in provenance. (B) GHI/(GHI+FD) separated into mudstone (red) and diamict (blue). This index is lithology dependent and is higher in diamicts than in mudstones. (C) Median thorium values for highstands and lowstands, demonstrating that thorium provenance depends on relative sea level change. (D) Median potassium/thorium ratios for highstands and lowstands, similarly demonstrating an association between provenance and sea level.

surfaces of erosion caused by glacial advance across the sea-floor, possibly during glacio-eustatic sea level fall (Cape Roberts Science Team, 1999) or perhaps unrelated to eustasy (Cape Roberts Science Team, 1998). The sequence stratigraphic interpretations of this paper and Cape Roberts Science Team (1999) fit the observed transgressive/regressive behavior of CRP-2 sediments. A weakness of the underlying model, however, is that it assumes the connection between glaciation and sea level which CRP originally had hoped to test: diamicts are attributed to both glacial processes and sea-level lowstands. In contrast, a relationship between transgressive/regressive cycles (or local sea-level changes) and glacial/interglacial periods is independently suggested by the following correlation: low-stand diamicts have both highland and lowland source provenance, whereas highstand muds have a highland source provenance.

Glacioeustasy can account for both the CRP-2 sea-level fluctuations and their apparent correlation with glacial/

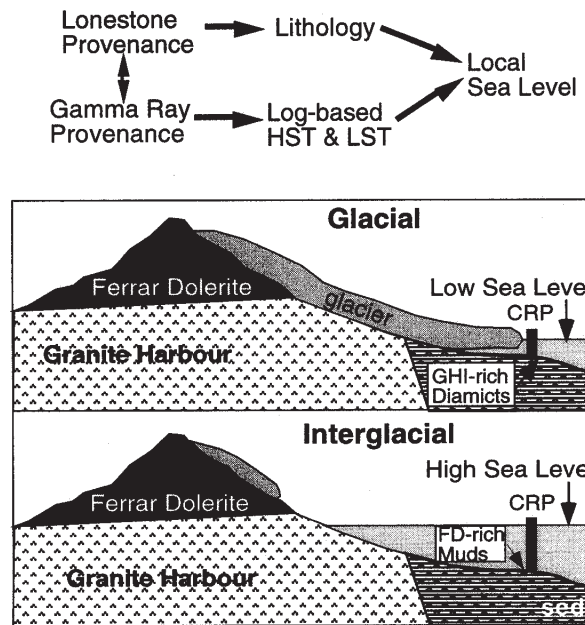


Fig. 6 - Top: flow chart of relationships based on correlations among datasets of figure 5. Bottom: cartoon cross-section views from the Transantarctic Mountains to beyond the CRP drill site, illustrating hypothesized relationships among provenance, glaciation, sea level, and lithology. Glacial: lowland erosion during glacial advance generates deposition of diamicts enriched in Granite Harbour Intrusives. Interglacial: ice volume is generally reduced, glacial erosion is confined to highlands, and muds enriched in Ferrar Dolerite are deposited at the drill site.

interglacial cycles. Miller et al. (1998) demonstrated correlations between New Jersey sequence boundaries and $\delta^{18}\text{O}$ increases indicating glacioeustasy back to 42 Ma. Within CRP, however, the sea-level significance of highstand and lowstand system tracts is uncertain. Sedimentary facies and molluscan fauna indicate >50 m changes in water depth within some sequences (Cape Roberts Science Team, 1999; Taviani et al., this volume), but little or no change in others (Strong and Webb, this volume). Some, perhaps many, of the CRP-2 sequences may be unrelated to sea level: glacial advance can scour and deposit "lowstand" diamicts in water depths of >50 m, followed by glacial retreat and "highstand" mud deposition in the same water depth (Cape Roberts Science Team, 1998, 1999). Thus it is possible that some of the highstand/lowstand cycles are sea-level induced whereas others are entirely caused by glacial processes.

Although the simple model of figure 6B is able to account for the correlations of figure 6A, the erosion, transport, and sedimentation processes of the sedimentary cycle are of course more complex in detail. The transport process is imperfectly coupled to erosion: glacially eroded sediments can be deposited in the lowlands, then remobilized by either fluvial outwash or later glacial advance. "Interglacial" periods can be characterized as time intervals of generally more restricted glacial extent than "glacial" periods, but presence of lonestones at CRP-2 indicates that these periods of reduced ice influence must include occasional glacial advance into the sea. Resulting ice-rafting supplies rare lonestones to offshore muds, in contrast to

the lonestone-rich diamicts deposited at the same site during glacial periods.

On the modern Mackay Glacier, supraglacial clasts contain a higher proportion of Ferrar Dolerite and may be ice-rafted more extensively than subglacial clasts (Powell, personal communication, 1999). This mechanism, however, accounts only for lonestone provenance. It cannot explain the observed correlation between bulk-rock thorium and both lonestones and systems tracts, because ice-rafting is not the main transport mechanism for highstand muds and sands. Furthermore, supraglacial clasts are typically much more angular than subglacial clasts (Barrett, 1980), but no pattern of greater angularity for Ferrar lonestones than for Granite Harbour lonestones has been identified (Cape Roberts Science Team, 1999; Talarico et al., this volume).

CONCLUSIONS

These CRP log analyses indicate that log-based detection of lithology and log units, though feasible and useful, is less fruitful than log-based delineation of sequences and provenance changes. The log-based sequence stratigraphy of CRP-2, based on a traditional sequence stratigraphic model, confirms and slightly modifies the core-based sequence stratigraphy of Cape Roberts Science Team (1999).

We have identified an association among thorium fluctuations, potassium/thorium ratios, provenance change, lithology, and systems tracts. The combination of these observations is consistent with the idea that during interglacial times highland sources are eroded and during glacial times both highlands and lowlands are eroded. Alternative hypotheses for - and further investigations of - relationships among provenance, glaciation, lithofacies, and sea level are needed. Other types of high-resolution provenance studies (whole-rock mineralogy and geochemistry, sand provenance, etc.) should be compared with systems tracts and with lithology variations.

ACKNOWLEDGEMENTS

We thank all members of the Cape Roberts Science Team for the open interchange of ideas that helps make the project so successful. We thank P. Kyle for allowing us to compare his geochemical data with our gamma-ray logs. This research was supported by the National Science Foundation (OPP-9418429).

REFERENCES

- Barrett P.J., 1980. The shape of rock particles, a critical review. *Sedimentology*, **27**, 291-303.
- Barrett P.J., Henrys S.A., Bartek L.R., Brancolini G., Busetti M., Davey F.J., Hannah M.J. & Pyne A.R., 1995. Geology of the margin of the Victoria Land basin off Cape Roberts, southwest Ross Sea. In: A.K. Cooper, P.F. Barker & G. Brancolini (eds.), *Geology and Seismic Stratigraphy of the Antarctic Margin*, *Antarctic Research Series*, **68**, AGU, Washington, 183-208.
- Barrett P.J., Pyne A.R. & Ward B.L., 1981. Modern sedimentation in McMurdo Sound, Antarctica. In: Oliver R.L., James P.R. & Jago J.B. (eds.), *Antarctic Earth Science*, Australian Academy of Science, Canberra, 550-555.
- Bridle I.M. & Robinson P.H., 1989. Diagenesis. In: Barrett P.J. (ed.), *Antarctic Cenozoic history from the CIROS-1 drillhole, McMurdo Sound*, *DSIR Bulletin*, **245**, 201-207.
- Brink J.D., 1999. Petrophysics and Log-based Sedimentology of the Cape Roberts Project, Antarctica. Univ. of Utah, *unpubl. M.S. thesis*, 183 pp.
- Brink J.D., Jarrard R.D., Krissek L.A. & Wilson T.J., 1998. Lonestone abundance and size variations in CRP-1 drillhole, Victoria Land Basin, Antarctica, *Terra Antartica*, **5**(3), 367-374.
- Cape Roberts Science Team, 1998. Initial Report on CRP-1, Cape Roberts Project, Antarctica. *Terra Antartica*, **5**(1), 187 pp.
- Cape Roberts Science Team, 1999. Studies from the Cape Roberts Project, Ross Sea, Antarctica, Initial Report on CRP-2/2A. *Terra Antartica*, **6**(1-2), 173 pp.
- Emery D. & Myers K.J. (eds.), 1996. *Sequence Stratigraphy*. Blackwell, Oxford U.K., 297 pp.
- Fielding C.R., Woolfe K.J., Howe J.A. & Lavelle M., 1998. Sequence stratigraphic analysis of CRP-1, Cape Roberts Project, McMurdo Sound, Antarctica, *Terra Antartica*, **5**(3), 353-361.
- Loutit T.S., Hardenbol J., Vail P.R. & Baum G.R., 1988. Condensed sections: the key to age determination and correlation of continental margin sequences. In: Wilgus C.K. et al., (eds), *Society of Paleontologists and Mineralogists Special Publication 42*, 183-213.
- Miller K.G., Mountain G.S., Browning J.V., Kominz M., Sugarman P.J., Christie-Blick N., Katz M.E. & Wright J.D., 1998. Cenozoic global sea level, sequences, and the New Jersey Transect: results from coastal plain and continental slope drilling. *Rev. Geophys.*, **36**, 569-601.
- Naish T.R. & Kamp P.J.J., 1997. Sequence stratigraphy of 6th order (41 k.y.) Pliocene-Pleistocene cyclothems, Wanganui Basin, New Zealand: a case for the regressive systems tract. *Geol. Sci. America Bull.*, **109**, 979-999.
- Niessen F., Jarrard R.D. & Bucker C., 1998. Log-based physical properties of the CRP-1 core, Ross Sea, Antarctica, *Terra Antartica*, **5**(3), 299-310.
- Niessen F. & Jarrard R.D., 1998. Velocity and porosity of sediments from CRP-1 drillhole, Ross Sea, Antarctica, *Terra Antartica*, **5**(3), 311-318.
- Sagnotti L., Florindo F., Verosub K.L., Wilson G.S. & Roberts A.P., 1998a. Environmental magnetic record of Antarctic palaeoclimate from Eocene-Oligocene glacial marine sediments, Victoria Land Margin. *Geophys. J. Internat.*, **134**, 653-662.
- Sagnotti L., Florindo F., Wilson G.S., Roberts A.P. & Verosub K.L., 1998b. Environmental magnetism of Lower Miocene strata from the CRP-1 core, McMurdo Sound, Antarctica, *Terra Antartica*, **5**(3), 661-668.
- Van Wagoner J.C., Mitchum R.M., Campion K.M. & Rahmanian V.D., 1990. *Siliciclastic Sequence Stratigraphy in Well Logs, Cores, and Outcrops: Concepts for High-Resolution Correlation of Time and Facies*, AAPG Methods in Exploration Series, No. 7, American Association of Petroleum Geologists, Tulsa, 55 pp.